

Self-assembly of aluminium-pillared clay on a gold support

Pegie Cool,^{*a} Abraham Clearfield,^b Vimala Mariagnanam,^b Laurel J. Mc. Ellistrem,^b Richard M. Crooks^b and Etienne F. Vansant^a

^aLaboratory of Inorganic Chemistry, Department of Chemistry, University of Antwerp, Universiteitsplein 1, 2610 Wilrijk, Belgium

^bDepartment of Chemistry, Texas A&M University, College Station, Texas 77843-32565, USA

Multilayer films of self-assembled aluminium Keggin ion pillared laponite and saponite have been grown layer-by-layer on a gold support. 4-Aminothiophenol (4-ATP) was used for anchoring the first clay layer on the gold surface. Subsequently layers of clay and Al pillar were adsorbed by dipping the substrate into the appropriate solutions. Characterization of the films was performed by X-ray photoelectron spectroscopy (XPS), IR spectroscopy (FTIR–ERS), ellipsometric thickness measurements and X-ray diffraction (XRD). XPS elemental analysis showed that both clay and pillar were present on the gold substrate. From the atomic film compositions, the charges on the Keggin ions were determined to be +3 and +5 for laponite and saponite, respectively. Ellipsometry and IR spectroscopy indicated gradual and regular growth for both films. Structural order in the synthesized films was demonstrated by X-ray diffraction. The interlayer free spacing (IFS) was found to be 6 Å by XRD, which corresponds to the increase in ellipsometric film thickness after each aluminium layer adsorption. Aluminium-pillared laponite films have been used as chemically sensitive films on surface acoustic wave (SAW) devices to measure the adsorption capacity of six volatile organic compounds (VOCs). The influences of the different terminal film layers and calcination-induced chemical changes on the extent of adsorption of the VOCs were investigated.

Pillared clays (PILCs) are a well known class of porous materials useful for catalytic and adsorption applications.^{1–3} In this study multilayer films of aluminium-pillared laponite and saponite were grown on a gold wafer by means of the alternate adsorption of clay and pillar on the support. The first step involved the reaction of a coupling agent between the first clay layer and the gold support. The gradual and regular growth of the films was evidenced by ellipsometry and FTIR–external reflectance spectroscopy (FTIR–ERS). X-Ray diffraction was utilised to show the structural order of the grown films. Atomic concentrations as determined by XPS allow the calculation of the positive charge on the Al₁₃ Keggin ions in the multilayer films. Gas adsorption experiments performed using surface acoustic wave (SAW) mass transducers clarify the gas adsorption properties of the films as a function of their top layer, thickness and calcination step.

Following conventional techniques, PILCs are synthesized by an exchange reaction of a pillaring solution containing large oligomeric hydroxy–metal cations (*e.g.* Al⁴⁺, Zr⁵⁺, Ti⁶⁺) with a smectite clay. The charge-compensating cations between the clay sheets are replaced by the oligomers. Upon calcination the polyoxycations are converted to the oxide form, creating a two-dimensional porous system. However, the porosity of these PILCs is still not what was expected because of the incomplete swelling of clay layers resulting in the interstratification of pillared and unpillared layers. Therefore, some reproducibility problems are often encountered. Theoretical studies based on geometrical models indicate aggregates of only fifteen and six parallel layers for Al-intercalated montmorillonite and laponite, respectively.^{7,8} Using these conventional methods the Al-pillaring of laponite results in an X-ray amorphous material, owing to non-parallel or random stacking of the small clay plates. Also for the larger sized clays, like saponite, the non-parallel stacking of plates is still important and results in poor crystallinity.

In this study a self-assembly method has been utilised in order to improve the pillaring of clays. More controllable pillaring can be achieved by a layer-by-layer deposition of clay and pillar. By means of the alternate adsorption of oppositely charged species, it becomes possible to grow multilayer films

on a solid support (*e.g.* Si or Au). Laponite clay, α -zirconium phosphate and layered metal-oxide semiconductors (LMOS) such as K₂Nb₆O₁₇^{2–} have been used as negative layers in previous studies.^{9–11} Polymeric or oligomeric cations utilised as positive species are bonded electrostatically to the negative layers. The ionic attraction between different layers forms the basis and stability of the film growth. The grown films can potentially be used as optical elements or sensors.¹²

Experimental

Materials and material preparation

The laponite RD was supplied by Laporte Inorganics. The idealised unit cell formula is: (Na_{0.5}·nH₂O)(Mg_{5.5}Li_{0.5})Si₈(OH)₄O₂₀ (*M_w* = 761) with a cation-exchange capacity (CEC) of 0.733 mequiv. g^{–1}.¹³

Calcium saponite was obtained from the Source Clay Minerals Repository of the Clay Minerals Society, Missouri, USA. The fraction <2 μ m was obtained by wet sedimentation. The clay was converted into the Na form by treatment with 1 mol dm^{–3} NaCl (3 \times), followed by washing the mixture until it was free of chlorine. The unit cell formula is as follows: Na_{0.88}Mg₆(Si_{7.1}Al_{0.72}Fe_{0.14})O₂₀(OH)₄ (*M_w* = 780) with a CEC of 1.13 mequiv. g^{–1}.

Gold substrates were obtained by thermal evaporation of 2000 Å Au over a 50 Å Ti adhesion layer on Si(100) wafers. After dicing the substrate to 2.5 \times 1.3 cm² pieces, the substrates were cleaned in an argon ion plasma (Harrick, model PDC-32G) for 1.5 min and rinsed in ethanol.

4-Aminothiophenol (4-ATP) was obtained from Aldrich and purified by vacuum sublimation prior to use.

Characterization techniques

A Seifert-Scintag PADII Powder diffractometer (Cu-K α radiation; 40 kV; 30 mA) was used to determine the order in the grown multilayer on the Au wafer.

FTIR–ERS measurements were made using a Digilab FTS-40 spectrometer equipped with a Harrick Scientific Seagull

reflection accessory and a liquid N₂-cooled MCT detector. An Au wafer immersed in a KI solution (2 mmol dm⁻³ in EtOH) for 10 min was used as the blank. All spectra are the sum of 256 individual scans (resolution 2 cm⁻¹) using p-polarized light at an 84° angle of incidence with respect to the Au substrate. All spectra were baseline corrected.

Multilayer thickness measurements were made using a Gaertner Scientific ellipsometer (model L116C). Data were collected using the 633 nm He-Ne laser line at a 70° incident angle, and assuming a refractive index of 1.46.

XP spectra were acquired using a Perkin-Elmer (PHI) Model 5500 spectrometer. In a typical XPS data acquisition, a pass energy of 29.3 eV, a step increment of 0.125 eV and a Mg anode power of 400 W were employed. Atomic compositions were calculated from peak areas using sensitivity factors provided in the software of the instrument.

Solution NMR spectra for ²⁷Al were recorded on a Varian XL-200 with a BB80S3 probe at 52.1 MHz. Chemical shifts were obtained in ppm referenced to external Al(H₂O)₆³⁺ in D₂O as derived from 0.1 mol dm⁻³ aqueous AlCl₃ solution.

SAW device measurements were made at 25 °C using two (98 MHz) ST-cut quartz oscillators housed in a custom-made flow system.¹⁴ Modified SAW devices were dosed with vapour-phase probe molecules mixed in N₂ at 25% of saturation (flow-rate=0.5 dm³ min⁻¹). The change in SAW device frequency (Δf) due to the adsorption of vapour-phase molecules is related to the mass loading per unit area (m_a) through the equation $\Delta f/f_0 = -kc_m f_0 m_a$, where, f_0 is the SAW resonance frequency (98 MHz), k is the fraction of the distance between the centres of the transducers covered by the Au film (0.65) and c_m is the mass sensitivity coefficient of the device (1.33 cm² g⁻¹ MHz⁻¹ for ST-cut quartz).^{15,16}

Procedures

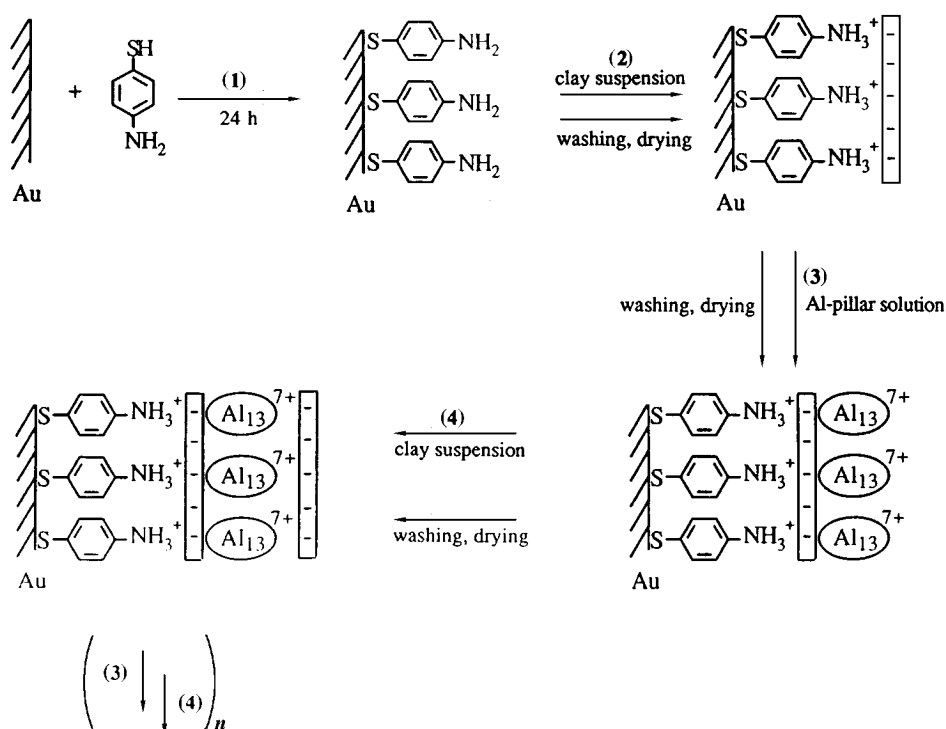
The procedure used to prepare the layered clay materials is represented in Scheme 1. Each cycle consists of two different steps, in which clay and pillar are adsorbed successively. Initially (step 1), the Au wafer is reacted with a coupling agent, 4-aminothiophenol (4-ATP). The reaction was carried out by immersing the gold wafer in a 1 mmol dm⁻³ solution of 4-

ATP in absolute ethanol for 24 h. The wafer was washed with EtOH and blown dry with N₂. Subsequently (step 2), the wafer was dipped for 15 min in a 0.2% clay suspension of laponite or saponite. Prior to use, the suspensions were sonicated overnight in a water-bath in order to obtain complete exfoliation of the clay. In the case of the saponite clay some flocculation was still observed. Therefore the centrifugate remaining after 2 min of centrifugation was used for layered-film preparation. For laponite, complete exfoliation of the clay was achieved by sonication and suspensions prepared in this way were used after acidification to a pH of 4 using 1 mol dm⁻³ HCl. At this pH, 4-ATP becomes protonated and attracts the negative clay plates. After reaction, the wafer was washed with deionised water and blown dry with N₂. In a following reaction (step 3), the wafer was dipped for 15 min in a 0.02 mol dm⁻³ Al pillar solution, followed by washing with deionised water and drying with N₂. The Al₁₃ pillar solution was prepared by dissolving 12 g of AlCl₃·6H₂O (0.05 mol) in 200 ml deionised water. To this solution 250 ml of 0.5 mol dm⁻³ NaOH (0.125 mol, molar ratio OH/Al=2.5) was added dropwise under vigorous stirring while heating at 80 °C for 3 h. After cooling, the solution was diluted and adjusted to a pH of 5.0. A ²⁷Al NMR spectrum showed a single peak at δ 63.5 indicating the presence of the Al₁₃ Keggin ion. In order to deposit the next clay layer (step 4), 0.2% clay suspensions adjusted to pH 6 with 1 mol dm⁻³ HCl were employed. The immersion time of the wafer with the clay suspension was limited to 15 min, following which the wafer was washed and dried with N₂. The last two steps (3 and 4) were repeated to grow multilayer films on the Au substrate by the alternate adsorption of oppositely charged species.

Results and Discussion

X-Ray photoelectron spectroscopy

The atomic compositions of the substrate (Au + ATP) and the grown multilayers of Al-pillared laponite and saponite after 30 cycles were determined by XPS analysis and the results are presented in Table 1.



Scheme 1

Table 1 Atomic compositions (%) as determined by XPS analysis

element	ATP ^a	laponite ^b	saponite ^c
Au	36.55	0.19	0.19
C	55.19	21.49	20.95
Si		10.81	9.79
O		52.40	52.13
Mg		6.43	7.01
Al		8.58	9.82
Na		0.10	0.11
N	4.19		
S	4.07		

^aATP monolayer on gold. ^bAl-pillared laponite film on gold after 30 cycles. ^cAl-pillared saponite film on gold after 30 cycles.

After the cycling process, the atomic compositions of Au and C detected on the surface decrease significantly owing to the presence of a thick clay multilayer on top of the substrate. The elements present in the saponite silicate layers (Si, O, Mg, Al) were detected. In the case of laponite, atomic concentrations of all elements (Si, O, Mg) except Li are determined. The reason is the low concentration and the low XPS sensitivity factor for Li. The presence of very small amounts of Na ions and large amounts of aluminium indicates that almost total exchange of the Na⁺ for Al polyoxycations has been attained. Calculations can be performed knowing the structural formulae, molecular masses (M_w) and CECs of both clays. The theoretically obtained values for the Si/Mg and Si/Al ratios are given in Table 2 and are compared to the experimental results obtained by XPS. For the Si/Al calculation, a total exchange of the CEC for the $[\text{Al}_{13}\text{O}_4(\text{OH})_{24+x}(\text{H}_2\text{O})_{12-x}]^{n+}$ ($n=7-x$; $M_w=1038.7$) is assumed, while the charge n on the Keggin ion varies ($n=3-7$). In the case of saponite, the contribution of Al present in the clay sheets was taken into account.

Good correlation between theory and experiment was obtained for Al₁₃ charges of +3 and +5 in the cases of laponite and saponite, respectively. The ideal literature formula for the Keggin ion requires a charge of +7; this value changes upon hydrolysis of the ion.^{17,18} For Al₁₃ intercalated in montmorillonite, pillar charges varying from +2.33 to +4 are obtained by performing theoretical calculations on the pillared material.⁷ A charge of +3.15 rather than the formal value of +7 has been reported by Jones and Purnell.¹⁹ For adsorption of Al₁₃ on saponite and hectorite, the average charges per Al are +0.4 and +0.2, respectively, as described by Schoonheydt *et al.*⁴ These latter values correspond to Al₁₃^{5.2+} on saponite and the lower charged Al₁₃^{2.6+} on hectorite, in close approximation to our data derived from XPS analysis (+5 and +3 respectively). A hydrolysis reaction on Al₁₃ involves a sequence of deprotonation steps occurring in solution and after adsorption on the clay layers. A higher hydrolysis degree upon exchange, forming lower charged Keggin ions is more likely to occur on hectorite and laponite than on saponite; hectorite

Table 2 Theoretical and experimental values as obtained by XPS for Si/Mg and Si/Al ratios for Al-pillared laponite and saponite

	theoretical	experimental
laponite		
Si/Mg	1.68	1.68
Al ₁₃ ⁿ⁺ , $n=3$; Si/Al	1.22	1.25
$n=7$; Si/Al	2.84	
saponite		
Si/Mg	1.37	1.40
Al ₁₃ ⁿ⁺ , $n=3$; Si/Al	0.62	
$n=5$; Si/Al	0.99	0.99
$n=7$; Si/Al	1.33	

and laponite are structurally identical and have a smaller charge density on their layers, compared to saponite.

IR spectroscopy

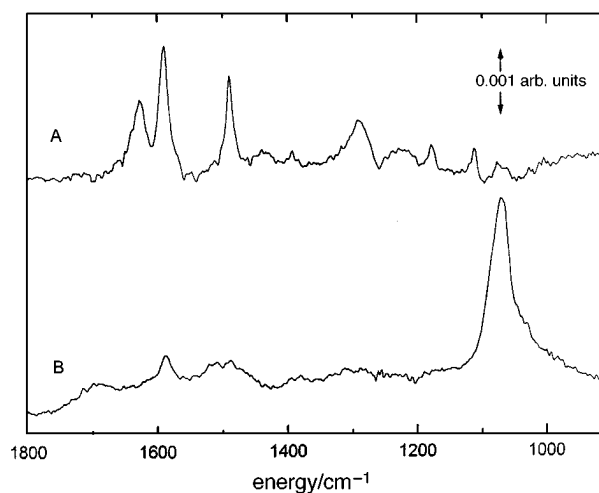
The growth of the film at initial stages of the cycling process has been investigated by FTIR-ERS measurements. Spectrum A in Fig. 1 shows a 4-ATP monolayer confined to the surface through a strong interaction between the Au and the sulfur atom of the thiol.²⁰

One can distinguish the peaks of the -NH₂ deformation (1625 cm⁻¹), the aromatic C=C stretch (1589, 1491 cm⁻¹) and the C-N stretching (1292 cm⁻¹). During the first step of the cycling process a pH of 4 for the clay suspensions was used in order to protonate the amino groups. In this way a positive layer charge is created on the Au substrate, which can serve to attract the anionic clay plates. In spectrum B it is seen that the attachment of a laponite layer on the organic ATP monolayer results in the disappearance of the -NH₂ peak, together with the appearance of the silicate peak (Si-O vibration at 1071 cm⁻¹).

The growth of the silicate peak at 1071 cm⁻¹ for the first eight cycles is clear for both laponite [Fig. 2(a)] and saponite [Fig. 2(b)]. The gradual increase in the peak height, which correlates with the number of clay layers, is shown in the insets. In the case of saponite it is almost linear.

Ellipsometry

The ellipsometrically determined thicknesses of both the laponite and saponite films indicate gradual and regular growth for the first eight cycles (Fig. 3). The thickness of the ATP monolayer on Au was determined to be 7 Å and this value was subtracted from the thicknesses shown in this plot. Each point is the result of three measurements obtained at different spots on the substrate, and they vary by a maximum of ±3 Å. This proves that the thicknesses of the multilayer films for both clay types are very homogeneous. It becomes apparent that the small plate size of laponite (300 Å), compared to that of saponite (10 000 Å), has no adverse effect on the homogeneity of the synthesized films. It is possible to calculate the amount of adsorbed clay and pillar per cycle by assuming complete coverage of the substrate by the clay, the plate sizes given above and the dimensions of the substrate. The numbers of clay sheets deposited on the substrate per cycle are then determined to be 3.61×10^{11} for laponite and 3.25×10^8 for saponite. If we further consider the number of plates per gram for laponite (4.28×10^{17}) and saponite (3.78×10^{14}),⁸ the above results indicate that 0.85 μg is adsorbed per cycle, irrespective

**Fig. 1** FTIR-ER spectra of 4-aminothiophenol on Au (A) and after protonation and subsequent deposition of a laponite layer (B)

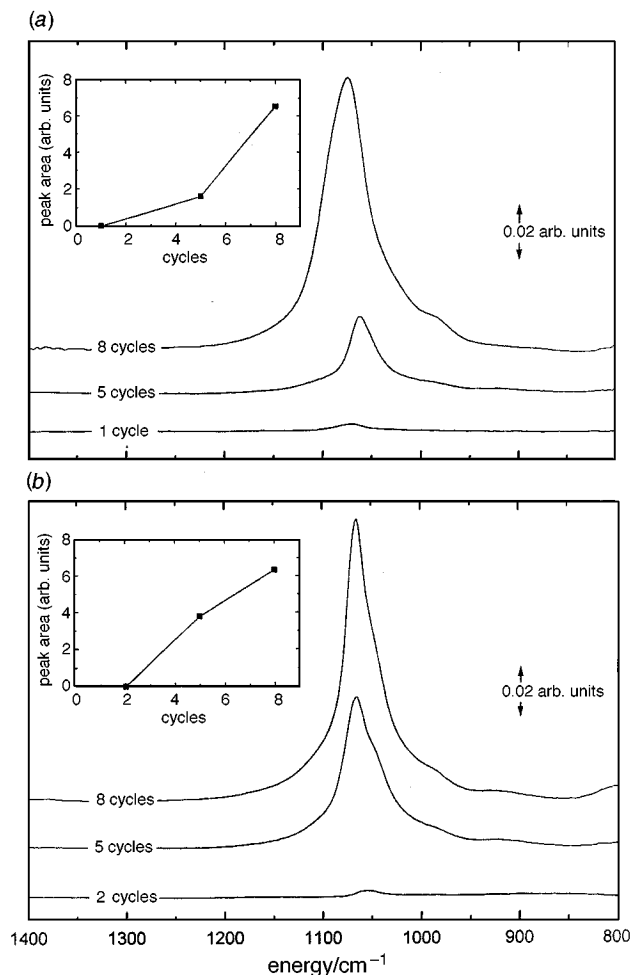


Fig. 2 FTIR-ER spectra of (a) pillared laponite on Au after 1, 5 and 8 deposition cycles, and (b) pillared saponite on Au after 2, 5 and 8 deposition cycles. The insets show the peak area *vs.* number of deposition cycles.

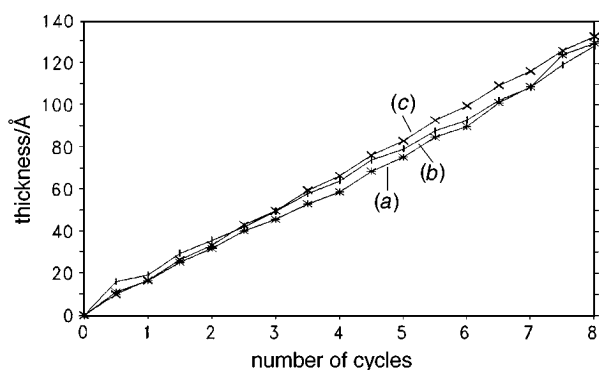


Fig. 3 Ellipsometric thickness as a function of the number of cycles for (a) laponite and (b) saponite; the calculated (theoretical) thickness is also shown (c)

of the clay type. After a total exchange of the CEC for Al_{13}^{3+} on laponite, and Al_{13}^{5+} on saponite, we calculate loadings of $0.21 \mu\text{g Al}_{13}$ per cycle. Consistent with our calculations, Fig. 3 shows a nearly identical evolution of film thickness as a function of layer number for both clays. Each curve consists of two different slopes that alternate depending on whether the clay or pillar is adsorbed. In the first step of each cycle a laponite or saponite monolayer with a thickness of 9.6 \AA adsorbs. As a following step in each cycle, Keggin ions are adsorbed onto the clay. Therefore, the increment in thickness must correspond to the Al_{13} dimensions. The original symmetry

of the Keggin ion is stated as a prolate spheroid with long and short axes of 9.5 and 7 \AA , respectively.²¹ The theoretical curve in Fig. 3 is calculated based on the clay layer thickness of 9.6 \AA and the smallest dimension of the Keggin ion (7 \AA axis). For both laponite and saponite the experimental curves closely approach the theoretical, and therefore we infer a flat orientation of Al_{13} between the clay sheets. More precisely, the mean increment in film thickness after each adsorption of Al pillars, as determined by ellipsometry, is *ca.* 6 \AA for both clays.

X-Ray diffraction

The ellipsometrically determined average interlayer free spacing (IFS) of 6 \AA can be compared to that derived from the XRD pattern (Fig. 4). The first broad peak in both patterns at a small 2θ value is due to the synthesized films on the substrate. All other diffractions at higher 2θ originate from the Au substrate itself (as determined from control experiments) and are of minor importance here. XRD does confirm the existence of structural order in the eight-layer films, although the diffraction peaks are very broad. By applying the Scherrer equation it becomes possible to estimate the number (N) of coherently diffracting clay layers along the c axis. The equation expresses the correlation between the number of parallel layers, N , and the 001 peak width at half height as determined by XRD.^{17,22} N is found to be 5 for both the Al-pillared laponite and the saponite film after eight cycles. The d_{001} values vary between 14.5 and 16.5 \AA for both clays. The average d_{001} value is 15.5 \AA , which corresponds to an IFS of 6 \AA after subtraction of the clay layer thickness. This indicates a small axis of only 6 \AA for the adsorbed Al_{13} pillars. Literature data suggest that the dimension of the Keggin ion should be larger: IFS values of 7 – 10 \AA have been obtained after Al pillaring.^{21,23,24} However, on the basis of theoretical calculations we conclude a cylindrical symmetry for the Keggin ion with a height of 9 \AA and a diameter of 6.32 \AA .⁷ This latter dimension is a better approximation to our experimentally observed spacing of 6 \AA . The washing procedure is also very important and crucial to obtain the typical 18 – 19 \AA d_{001} value conforming to the dimension of the Keggin ion.^{4,13} The Keggin ions might not be the only intercalated Al species while washing causes chemical changes of the intercalated Al products. During the washing the pH is raised slightly, allowing polymerization and reorganization of Al species in the interlayer space. For Al-hectorite and Al-saponite, d_{001} spacings of 14.6 and 13 \AA , respectively, have been reported before washing. These values increased by 3.2 and 5.5 \AA respectively after four separate washes.⁴ The short washing procedure as part of our cycling process accounts for the limited polymerization of Al_{13} on the clay.

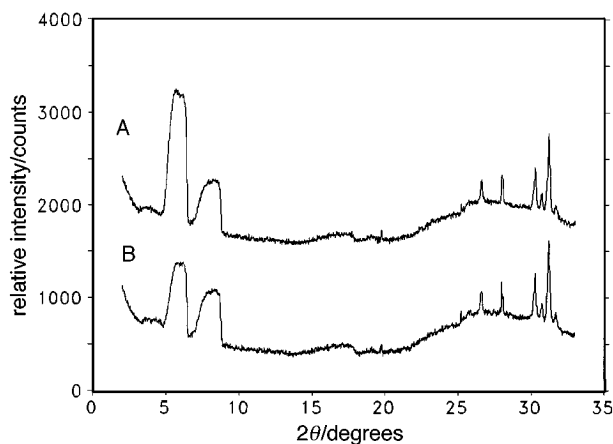


Fig. 4 X-Ray diffractograms for pillared laponite (A) and pillared saponite (B) on Au after 8 deposition cycles

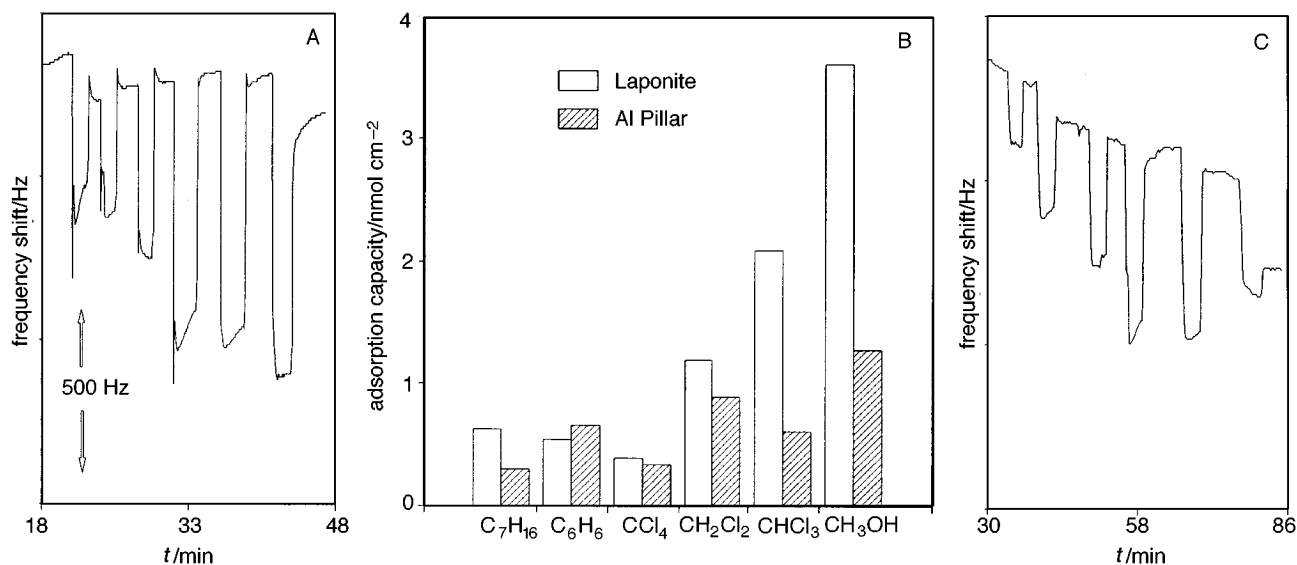


Fig. 5 Results of gas-dosing experiments performed on a four-layer pillared laponite film having either clay or Al pillar on top. Data were obtained using a mass-sensitive SAW device. Parts A and C represent the frequency shifts as a function of time for films terminating in clay and pillar, respectively. Part B gives the adsorption capacities in nmol cm^{-2} for the different gases. The order of gas dosing in parts A and C is the same as shown in B. Vapours were present at 25% of saturation.

VOC adsorption

To determine the Al-pillared laponite film porosity, adsorption measurements of six organic vapours were performed using surface acoustic wave (SAW) mass sensors.^{15,16} Prior to vapour adsorption all films were degassed at 120 °C for 4 h in a vacuum oven. We determined the dependence of the extent of vapour adsorption as a function of the chemical composition of the top layer of the film, the film thickness and the calcination step. The SAW device frequency shifts as a function of time for adsorption of the six volatile organic compounds (VOCs) shown in Fig. 5B on Al-PILC films terminated in either laponite or pillar are shown in Fig. 5A and C, respectively.

Negative frequency shifts correlate to an increase in adsorbed mass. It can be seen that most of the adsorptions are reversible processes since the frequency returns to baseline upon purging of the films with pure N₂ (except for a temperature-induced drift, which is especially apparent in Fig. 5C). Only methanol remains irreversibly bound to the film to an appreciable extent. This effect is more significant when the film is terminated in Al pillars (Fig. 5C). This result is consistent with chemical intuition that suggests that alcohols will interact strongly *via* hydrogen bonding with the hydroxy groups of the Al₁₃ Keggin ions. In Fig. 5B the frequency shifts have been converted to mass loading per unit area (in units of nmol cm^{-2}) to remove the molecular mass bias. The clay-terminated film nearly consistently adsorbs more VOC than the Al-terminated films. This effect is most apparent in the cases of polar gas molecules like CH₂Cl₂, CHCl₃ and CH₃OH. The enhanced adsorption of the polar Cl-containing molecules, CH₂Cl₂ and CHCl₃, on the laponite layer can be explained by interaction with Na⁺ ions adsorbed to the film, imparting electrical neutrality to the system. The higher amount of adsorbed methanol in the case of a clay top layer is not only due to its polarity but also due to an induced swelling of the Al-pillared film on the Au support.

The swelling of films upon methanol adsorption becomes clear when films with different thicknesses are used as substrates. Fig. 6 shows the amount of VOC adsorbed as a function of thickness for laponite-terminated films. The increasing level of CH₃OH adsorption with the number of cycles can be explained by swelling effects of the pillared clay films. Adsorption takes place on the external surface area, and penetration into the porous system allows adsorption on the

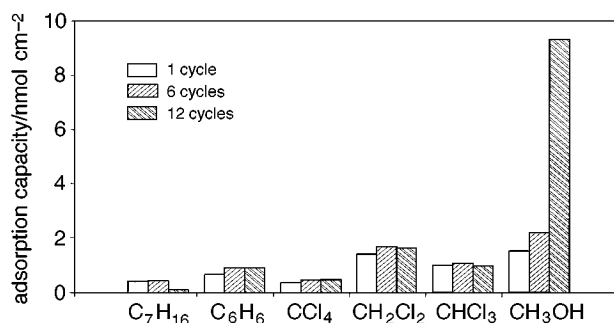


Fig. 6 Adsorption capacities of organic vapours on pillared laponite films after 1, 6 and 12 cycles with clay on top

internal surface area as well. Moreover, this penetration will be easier for the thicker twelve-cycled film compared to the well ordered thinner films because of a higher degree of disorder in the upper film layers.

The influence of a calcination step on VOC adsorption has also been investigated. A pillared clay film after four cycles with Al pillars on top was heated at a rate of 5 °C min⁻¹ to 300 °C and kept for 2 h at this temperature. The results of this experiment are shown in Fig. 7. For the apolar molecules (C₇H₁₆, C₆H₆, CCl₄) an increase in mass loading upon calcination is observed, while for the polar gases (CH₂Cl₂, CHCl₃, CH₃OH) the reverse occurs. We interpret this result in terms of chemical transformations that occur in the films during

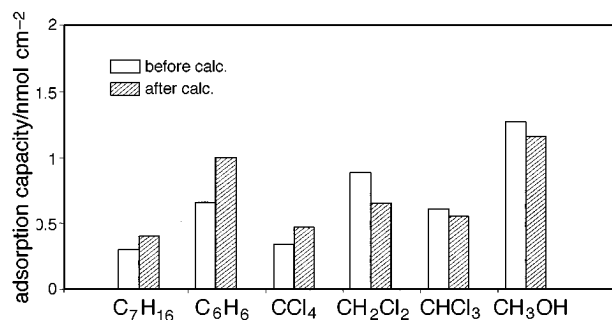


Fig. 7 Adsorption capacities of organic vapours on a pillared laponite film with the Al pillars as the top layer, before and after calcination

calcination; specifically, a change in charge on the Al₁₃ pillars. That is, during calcination, the Keggin ions are converted into the Al₂O₃ form, decreasing the positive charge on the Al overlayer. A weaker electronic interaction of this layer with the polar Cl-containing molecules leads to a decrease in adsorption. There will be less H₂O adsorbed onto the Al layer after calcination, resulting in a higher adsorption of the apolar molecules onto the film.

Summary and Conclusion

This study shows that by a self-assembly method it becomes possible to grow homogeneous films of Al-pillared laponite and saponite on a Au support. Protonated 4-aminothiophenol serves as the anchoring molecule between the Au substrate and the first clay layer. Cycling is performed by adsorbing clay and pillar layers successively during a 15 min contact time of the respective solutions with the substrate. After sonication of the clay suspensions to give totally exfoliated solutions, clay monolayers can be adsorbed with each cyclisation step. The films grow layer-by-layer as evidenced by FTIR-ERS and ellipsometry studies. XPS revealed the atomic compositions of the films. A comparison of the calculated and experimentally determined Si/Mg and Si/Al ratios allows us to estimate the Al₁₃ pillar charge. For laponite the charge on the Keggin ion is +3, while for saponite a charge of +5 results. These results are in close agreement with literature data. The average for the interlayer free spacing of the Al-pillared laponite and saponite is determined to be 6 Å by XRD and corresponds to the increment in film thickness after each Al layer adsorption, as measured by ellipsometry. We interpret this result in terms of a flat orientation of the spheroidal Al₁₃ pillars between the layers. The short washing procedure is a possible explanation for the reduced polymerization of Al₁₃ on the clay layers, resulting in a small diameter of 6 Å. Finally, VOC adsorption data measured by SAW devices are consistent with the top layer of the film and the film thickness. Calcination also influences the adsorption capacity. In the case of methanol the adsorption process becomes irreversible owing to swelling effects of the pillared clay.

P. C. acknowledges the NFWO/FNRS for financial support as research assistant and thanks the Fulbright Program for the educational exchange between the University of Antwerp and Texas A&M University. A. C. wishes to acknowledge support of this study by the National Science Foundation through Grant No. DMR-9407899. R. M. C., V. M. and L. J. Mc. E. acknowledge support from the US National Science Foundation (CHE-9313441).

References

- 1 T. J. Pinnavaia, *Science*, 1983, **220**, 365.
- 2 *Catal. Today*, Special Issue on Pillared Clays, 1988, vol. 2.
- 3 A. Molinard and E. F. Vansant, *Adsorption*, 1995, **1**, 49.
- 4 R. A. Schoonheydt, H. Leeman, A. Scorpion, I. Lenotte and P. Grobet, *Clays Clay Miner.*, 1994, **42**, 518.
- 5 K. Ohtsuka, Y. Hayashi and M. Suda, *Chem. Mater.*, 1993, **5**, 1823.
- 6 J. Sterte, *Clays Clay Miner.*, 1986, **34**, 658.
- 7 N. Maes, I. Heylen, P. Cool, M. De Bock, C. Vanhoof and E. F. Vansant, *J. Porous Mater.*, 1996, **3**, 47.
- 8 P. Cool, N. Maes, I. Heylen, M. De Bock and E. F. Vansant, *J. Porous Mater.*, 1996, **3**, 157.
- 9 E. R. Kleinfeld and G. S. Ferguson, *Science*, 1994, **265**, 370.
- 10 S. W. Keller, K. Hyuk-Nyun and T. E. Mallouk, *J. Am. Chem. Soc.*, 1994, **116**, 8817.
- 11 G. S. Ferguson and E. R. Kleinfeld, *Adv. Mater.*, 1995, **7**, 414.
- 12 G. Cao, H-G. Hong and T. E. Mallouk, *Acc. Chem. Res.*, 1992, **25**, 420.
- 13 R. A. Schoonheydt, J. Van Den Eynde, H. Tubbax, H. Leeman, M. Stuyckens, I. Lenotte and W. E. E. Stone, *Clays Clay Miner.*, 1993, **41**, 598.
- 14 H. C. Yang, D. L. Dermody, C. Xu, A. J. Ricco and R. M. Crooks, *Langmuir*, 1996, **12**, 726.
- 15 R. C. Thomas, L. Sun, R. M. Crooks and A. J. Ricco, *Langmuir*, 1991, **7**, 620.
- 16 H. Wohltjen, *Sens. Actuators*, 1984, **5**, 307.
- 17 A. Molinard, PhD Thesis, University of Antwerp, 1994.
- 18 D. E. W. Vaughan, *Catal. Today*, 1988, **2**, 187.
- 19 J. R. Jones and J. H. Purnell, *Catal. Lett.*, 1993, **18**, 137.
- 20 R. G. Nuzzo and D. L. Allare, *J. Am. Chem. Soc.*, 1983, **105**, 4481.
- 21 A. Clearfield and B. D. Roberts, *Inorg. Chem.*, 1988, **27**, 3237.
- 22 O. Braddell, R. C. Barklie and D. H. Doff, *Clay Miner.*, 1990, **25**, 15.
- 23 M. Tokarz and J. Shabtai, *Clays Clay Miner.*, 1985, **33**, 89.
- 24 R. A. Schoonheydt and H. Leeman, *Clay Miner.*, 1992, **27**, 249.

Paper 6/06129J; Received 5th September, 1996